

## Mechanical Properties of ZTA-Cr<sub>2</sub>O<sub>3</sub> Ceramic Composites Prepared with Nano and Micron Sized of Cr<sub>2</sub>O<sub>3</sub> Powder on Different Ratios

Uğur USTA<sup>1</sup>, Betül KAFKASLIOĞLU YILDIZ<sup>2\*</sup>

<sup>1</sup>Sivas University of Science and Technology, Institute of Graduate Studies, Defense Technology Program, 58000, Sivas

<sup>2</sup>Sivas University of Science and Technology, Faculty of Engineering and Natural Sciences, Metallurgical and Materials Engineering Department, 58000, Sivas

<sup>1</sup><https://orcid.org/0000-0002-8140-0916>

<sup>2</sup><https://orcid.org/0000-0002-6527-2918>

\* Corresponding author: bkyildiz@sivas.edu.tr

### Research Article

#### Article History:

Received: 27.03.2023

Accepted: 19.07.2023

Published online: 20.12.2023

#### Keywords:

ZTA

Cr<sub>2</sub>O<sub>3</sub>

Mechanical properties

Pressureless sintering

### ABSTRACT

In this study, the effect of Cr<sub>2</sub>O<sub>3</sub> addition in different powder sizes on the densification and mechanical properties (elastic modulus, hardness and flexural strength) of ZTA composites were investigated. Nano and micron sized of Cr<sub>2</sub>O<sub>3</sub> powder were added to the ZTA composite separately in different weight ratios (0.3, 0.6 and 1.0%) and uniaxially dry pressing right after pressureless sintering at 1650°C/2 h in the air used as processing procedure. X-ray diffraction method was used to verify the crystal structures and formed phases in the sintered samples. SEM and SEM-EDS analysis were carried out to evaluate the microstructures and identify the existence of elements after the solid solution formation of Al<sub>2</sub>O<sub>3</sub>-Cr<sub>2</sub>O<sub>3</sub>, respectively. The monotonic equibiaxial flexural strength test was performed to obtain fracture strength values and Vickers indentation method was used to measure the hardness. The relative density values of all the composites were close to each other for the Cr<sub>2</sub>O<sub>3</sub> containing composites. A slight decrease in both densification and elastic modulus was observed with the addition of Cr<sub>2</sub>O<sub>3</sub> due to the evaporation problem. Also, the addition of Cr<sub>2</sub>O<sub>3</sub> did not have a serious effect on the hardness of the ZTA composites. The main effect of Cr<sub>2</sub>O<sub>3</sub> addition on ZTA composites was seen for flexural strength. Compared to the ZTA, a nearly 7% increase in strength was obtained for 0.6% Cr<sub>2</sub>O<sub>3</sub> containing composite prepared with micron sized Cr<sub>2</sub>O<sub>3</sub> powder due to the generated compressive stresses in the grain boundary caused by solid solution formation. ZTA composites containing 0.6% Cr<sub>2</sub>O<sub>3</sub> with high strength value can be used as an alternative material to ZTA composites for structural applications.

## Farklı Oranlarda Nano ve Mikron Boyutlu Cr<sub>2</sub>O<sub>3</sub> Tozu İle Hazırlanan ZTA-Cr<sub>2</sub>O<sub>3</sub> Seramik Kompozitlerin Mekanik Özellikleri

### Araştırma Makalesi

#### Makale Tarihiçesi:

Geliş tarihi: 27.03.2023

Kabul tarihi: 19.07.2023

Online Yayınlanma: 20.12.2023

#### Anahtar Kelimeler:

ZTA

Cr<sub>2</sub>O<sub>3</sub>

Mekanik özellikler

Basınçsız sinterleme

### ÖZ

Bu çalışmada, farklı toz boyutlarında Cr<sub>2</sub>O<sub>3</sub> ilavesinin ZTA kompozitlerinin yoğunlaştırma ve mekanik özelliklerine (elastik modülü, sertlik ve eğilme mukavemeti) etkisi incelenmiştir. Üretim prosedürü olarak nano ve mikron boyutunda Cr<sub>2</sub>O<sub>3</sub> tozu farklı ağırlık oranlarında (% 0,3, 0,6 ve 1,0) ZTA kompozite ayrı ayrı ilave edilmiştir ve tek eksenli kuru preslemeye hemen sonra havada 1650°C/2 saat basınçsız sinterleme yapılmıştır. Sinterlenmiş numunelerde kristal yapıları ve oluşan fazları doğrulamak için X-ışını kırınım yöntemi kullanılmıştır. Al<sub>2</sub>O<sub>3</sub>-Cr<sub>2</sub>O<sub>3</sub> katı çözelti oluşumundan sonra mikroyapıları değerlendirmek ve elementlerin

varlığını belirlemek için sırasıyla SEM ve SEM-EDS analizleri yapılmıştır. Kırılma mukavemet değerlerini elde etmek için monotonik eşikieksenli eğilme mukavemet testi, sertliği ölçmek için Vickers iz yöntemi kullanılmıştır.  $\text{Cr}_2\text{O}_3$  içeren kompozitler için tüm kompozitlerin relatif yoğunluk değerleri birbirine yakın çıkmıştır.  $\text{Cr}_2\text{O}_3$  ilavesi ile buharlaşma probleminin dolayı hem yoğunlaştırma hem de elastisite modülünde hafif bir düşüş gözlenmiştir. Ayrıca  $\text{Cr}_2\text{O}_3$  ilavesinin ZTA kompozitlerinin sertliği üzerinde ciddi bir etkisi olmamıştır.  $\text{Cr}_2\text{O}_3$  ilavesinin ZTA kompozitler üzerindeki ana etkisi eğilme mukavemeti için görülmüştür. Mikron boyutunda  $\text{Cr}_2\text{O}_3$  tozu ile hazırlanan % 0,6  $\text{Cr}_2\text{O}_3$  içeren kompozitte, katı çözelti oluşumundan dolayı tane sınırlarında oluşan basma gerilmeleri nedeniyle ZTA'ya göre yaklaşık %7'lik mukavemet artışı elde edilmiştir. Yüksek mukavemet değeri ile %0,6  $\text{Cr}_2\text{O}_3$  içeren ZTA kompozitleri yapısal uygulamalar için ZTA kompozitlere alternatif bir malzeme olarak kullanılabilir.

**To Cite:** Usta U., Kafkaslıoğlu Yıldız B. Mechanical Properties of ZTA- $\text{Cr}_2\text{O}_3$  Ceramic Composites Prepared with Nano and Micron Sized of  $\text{Cr}_2\text{O}_3$  Powder on Different Ratios. Osmaniye Korkut Ata Üniversitesi Fen Bilimleri Enstitüsü Dergisi 2023; 6(Ek Sayı): 315-327.

## Introduction

Zirconia toughened alumina (ZTA) composite is a very popular material where zirconia particles are distributed in the alumina matrix as a second distinct phase (Weimin et al., 2008; Hassan et al., 2015). Zirconia has three crystallographic structures, monoclinic (m), tetragonal (t) and cubic (c) up to temperature. The transformation of pure zirconia from a tetragonal to a monoclinic structure occurs at around 950°C that results in 4% volume expansion (Tuan et al., 2002). Destructive phase transformation should be hindered for technological applications at the same time as the high-temperature forms of  $\text{ZrO}_2$ , tetragonal (t) and cubic (c) be supposed to become stable at room temperature (Moradkhani and Baharvandi, 2018). It is performed by adding appropriate oxide additives such as CaO,  $\text{Y}_2\text{O}_3$ , MgO,  $\text{CeO}_2$  and lanthanide oxides (Hassan et al., 2015).  $\text{Y}^{3+}$  in  $\text{Y}_2\text{O}_3$  can restrain  $c \rightarrow t \rightarrow m$  transformation and lower transformation temperature as the most used stabilizer of  $\text{ZrO}_2$  (Azhar et al., 2010). Also, the content of  $\text{Y}_2\text{O}_3$  has a distinct inhibition effect on transformation, which allows the metastable t- $\text{ZrO}_2$  phase to be present (Chevalier et al., 2009). As an important toughening mechanism, stress-induced  $t \rightarrow m$  phase transformation leads to an increase in fracture toughness in ZTA composites named transformation toughening (Weimin et al., 2008). Additionally, the  $\text{ZrO}_2$  phase allows for to restriction of abnormal grain growth of the  $\text{Al}_2\text{O}_3$  matrix through the pinning effect (Tuan et al., 2008). The pinning effect can result in the reduction of flaw size in the composite which can cause fracture strength enhancement. These improvements in the physical properties make ZTA materials favourable for critical structural applications that necessitate high mechanical properties such as armour (Kafkaslıoğlu Yıldız and Tür, 2021).

Chromia ( $\text{Cr}_2\text{O}_3$ ) is also an additive possibly able to increase the mechanical properties of  $\text{Al}_2\text{O}_3$  ceramics (Manshor et al., 2017). After the addition of  $\text{Cr}_2\text{O}_3$  into an  $\text{Al}_2\text{O}_3$ , a complete substitutional solid solution forms on the full range of compositions at high temperatures ( $T > 1000^\circ\text{C}$ ), as a result of  $\text{Al}_2\text{O}_3$  and  $\text{Cr}_2\text{O}_3$  are sesquioxides with the same corundum structure. Nevertheless,  $\text{Cr}_2\text{O}_3$  ceramics are not stable in a sintering atmosphere with high oxygen partial pressure that vapors of gaseous species

for instance  $\text{Cr}_2\text{O}_3$  appear above  $1000^\circ\text{C}$  (Nath et al., 2016). The solid solution formation promotes high chemical stability and refractoriness (Li et al., 1999). The hardness, fracture toughness and fracture strength of  $\text{Al}_2\text{O}_3$  could increase after  $\text{Cr}_2\text{O}_3$  addition (Azhar et al., 2012). It is stated that the matrix grains turn larger with bimodal size distribution in a specific content up to the production method therefore the fracture toughness is improved (Riu et al., 2000).

Although the research about  $\text{Al}_2\text{O}_3$ - $\text{Cr}_2\text{O}_3$  and ZTA has been done comprehensively for more than 20 years, the investigations were evaluated separately and the studies about mechanical properties of  $\text{Cr}_2\text{O}_3$  containing ZTA composites are less (Manshor et al., 2016; Xia et al., 2016; Azhar et al., 2012; Arahori and Whitney, 1988). Considering the positive effects of both  $\text{ZrO}_2$  and  $\text{Cr}_2\text{O}_3$  on the mechanical properties of  $\text{Al}_2\text{O}_3$  materials, it is remarkable to look at the simultaneous effect of these two additives. By combining the characteristic properties of different ceramic components, a specific composite with better properties can be produced. Azhar et al. studied the effects of  $\text{Cr}_2\text{O}_3$  addition on the mechanical properties, microstructure and wear performance of ZTA cutting inserts. They obtained an increase in the fracture toughness from  $4.41 \text{ MPa}\cdot\text{m}^{1/2}$  to  $4.73 \text{ MPa}\cdot\text{m}^{1/2}$  and the highest Vickers hardness as 16.06 GPa for 0.6 wt%  $\text{Cr}_2\text{O}_3$  addition among all the compositions (0, 0.2, 0.4, 0.6, 0.8, 1.0 wt%  $\text{Cr}_2\text{O}_3$ ) (Azhar et al., 2012). Arahori and Whitney studied the hardness, toughness and bending strength of  $(\text{Al}_2\text{O}_3 - \text{Cr}_2\text{O}_3) - 10 \text{ vol}\% \text{ ZrO}_2$  composites prepared with hot pressing and the maximum hardness was obtained for 10 wt%  $\text{Cr}_2\text{O}_3$  as nearly 16.5 GPa (Arahori and Whitney, 1988).

The purpose of this research is to investigate the elastic modulus, hardness and flexural strength of ZTA- $\text{Cr}_2\text{O}_3$  ceramic composites prepared separately with nano and micron sizes of  $\text{Cr}_2\text{O}_3$  powder on different weight ratios (0.3, 0.6, 1 wt%). It is stated that the distribution of the  $\text{Cr}_2\text{O}_3$  dopant into the matrix before dissolving will be beneficial to make it play a positive role in the solid solution formation and densification (Xia et al., 2016). Unlike the literature studies, the effect of  $\text{Cr}_2\text{O}_3$  powder size on the relevant mechanical properties of ZTA composites is in the foreground.

## Material and Method

$\alpha$ - $\text{Al}_2\text{O}_3$  (99.8%, 0.5  $\mu\text{m}$ , Almatix CT3000 LS SG, Germany), YSZ (3 mol%  $\text{Y}_2\text{O}_3$  stabilized  $\text{ZrO}_2$ , <0.5  $\mu\text{m}$ , MSE Tech Co. Ltd, Turkey), micron-sized  $\text{Cr}_2\text{O}_3$  (99%, 1  $\mu\text{m}$ , Nanografi, Turkey), nano-sized  $\text{Cr}_2\text{O}_3$  (99.5%, 55 nm, Nanografi, Turkey), polyacrylic acid as a dispersant (MSE Tech Co. Ltd., Turkey), polyvinyl alcohol as a binder (Sigma Aldrich) and glycerol as plasticizer (Sigma Aldrich) are the raw materials.  $\alpha$ - $\text{Al}_2\text{O}_3$ , YSZ and  $\text{Cr}_2\text{O}_3$  powder (micron and nano-sized, separately) were weighed in proper quantities as 5 wt% YSZ in every composite and 0.3, 0.6, and 1 wt% for  $\text{Cr}_2\text{O}_3$ , respectively. The  $\text{Cr}_2\text{O}_3$  ratios were determined by considering the literature studies (Azhar et al., 2012; Kafkaslıoğlu Yıldız et al., 2019). The weighted powders and polyacrylic acid (0.5% of total weight) were ball milled in distilled water for 24 h. Before the drying procedure, 3 wt% binder solution was poured into the ball-milled slurry and dried while stirring on a hot plate. The dried composite powder was crushed and sieved to 90  $\mu\text{m}$  for granulation. Green pellets were pressed in a 35 mm diameter of

cylindrical mould uniaxially at 50 MPa. The binder burn-out process was completed at 600°C/1 h at the beginning of the sintering. All the prepared green pellets were pressureless sintered at 1650°C for 2 h in the air atmosphere in a Lenton<sup>®</sup> furnace. ZTA composite without Cr<sub>2</sub>O<sub>3</sub> additive was also prepared under the same conditions for comparison.

The sintered specimens were firstly ground by using a lapping machine for both smoothing the surfaces and equalizing the thicknesses of the specimens then again ground with 1200 and 2000 grit SiC abrasive papers for mechanical tests. The bulk densities of the specimens were calculated as a volumetric density by the direct measurement of weight and dimensions. Theoretical densities of the composites were found by using the rule of mixtures to estimate the relative densities from the theoretical densities of the pure Al<sub>2</sub>O<sub>3</sub>, Cr<sub>2</sub>O<sub>3</sub>, and YSZ which are 3.98, 5.22, and 6.10, respectively. X-ray Diffraction (XRD) (Bruker<sup>®</sup> D8 Advance) was used at a scanning rate of 4°/min from 10° to 90° using Cu-K $\alpha$  ( $\lambda$  =1.5406 Å, 40 kV, 40 mA) in order to identify the present phases and crystal structures of the ceramic composites. The sintered specimens were thermally etched at 1550°C for 90 min in the air for microstructural observation and the analysis was carried out by using scanning electron microscopy (SEM, TESCAN Mira3 XMU) at accelerating voltage of 15 kV equipped with Energy Dispersive Spectroscopy (EDS). The matrix grain size of the composites was estimated by using the linear intercept method by counting more than 100 intercepts. The elastic modulus values were found by using an impulse excitation technique to disc ceramic specimens according to ASTM E 1876 standard in GrindoSonic<sup>®</sup> Mk5 machine with software. The monotonic equibiaxial flexural test method according to ASTM C 1499 standard was used to measure the bending strength of the ceramic composites with the Instron<sup>®</sup> 5569 device and twelve specimens of each composite was tested. In the strength tests, the displacement rate was set as 0.3 mm/min. The Vickers indentation method was used to measure the hardness of the composites under a 5 kg load for 10 s with an Instron<sup>®</sup> Wolpert Testor 2100 machine fitted with a diamond pyramid indenter.

## Results and Discussion

X-ray diffraction patterns of the ZTA and ZTA-Cr<sub>2</sub>O<sub>3</sub> composites after sintering prepared with 1  $\mu$ m Cr<sub>2</sub>O<sub>3</sub> powder are shown in Figure 1. Both the  $\alpha$ -Al<sub>2</sub>O<sub>3</sub> corundum phase and t-YSZ (tetragonal yttria-stabilized ZrO<sub>2</sub>) phase were detected. The names of the composites are abbreviated as given in the Figure. In short, A5Z means Al<sub>2</sub>O<sub>3</sub> containing 5 wt% ZrO<sub>2</sub> and A5Z0.3C means Al<sub>2</sub>O<sub>3</sub> containing 5wt% ZrO<sub>2</sub> and 0.3 wt% Cr<sub>2</sub>O<sub>3</sub>. The presence of monoclinic ZrO<sub>2</sub> was not detected in the patterns. Al<sub>2</sub>O<sub>3</sub> and Cr<sub>2</sub>O<sub>3</sub> have the same corundum crystal structure, no separate phase was identified after Cr<sub>2</sub>O<sub>3</sub> addition to the composite due to the solid solution formation. The formation of complete substitutional solid solution in corundum structure makes challenging to recognize the peak of Cr<sub>2</sub>O<sub>3</sub> as a distinct phase (Manshor et al., 2016). Also, XRD patterns of the pure ZTA and ZTA-Cr<sub>2</sub>O<sub>3</sub> composites after sintering prepared with nano Cr<sub>2</sub>O<sub>3</sub> powder are seen in Figure 2. There was no other

phase different from the phases in the XRD pattern of the composite prepared with micron powder. The letter “N” used in the abbreviation means prepared from nano  $\text{Cr}_2\text{O}_3$  powder.

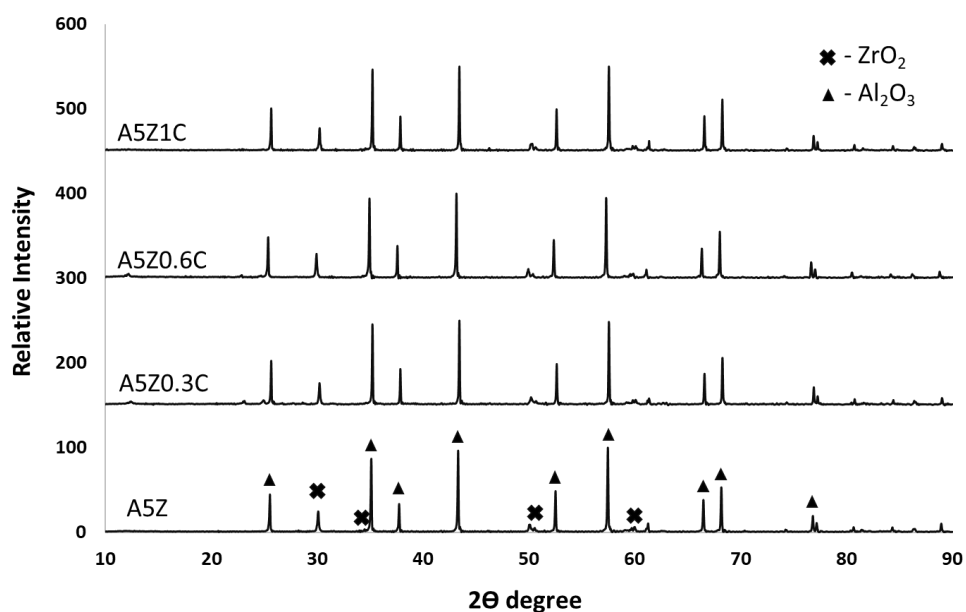


**Figure 1.** XRD patterns of the ZTA and ZTA- $\text{Cr}_2\text{O}_3$  composites after sintering prepared with 1  $\mu\text{m}$   $\text{Cr}_2\text{O}_3$ .

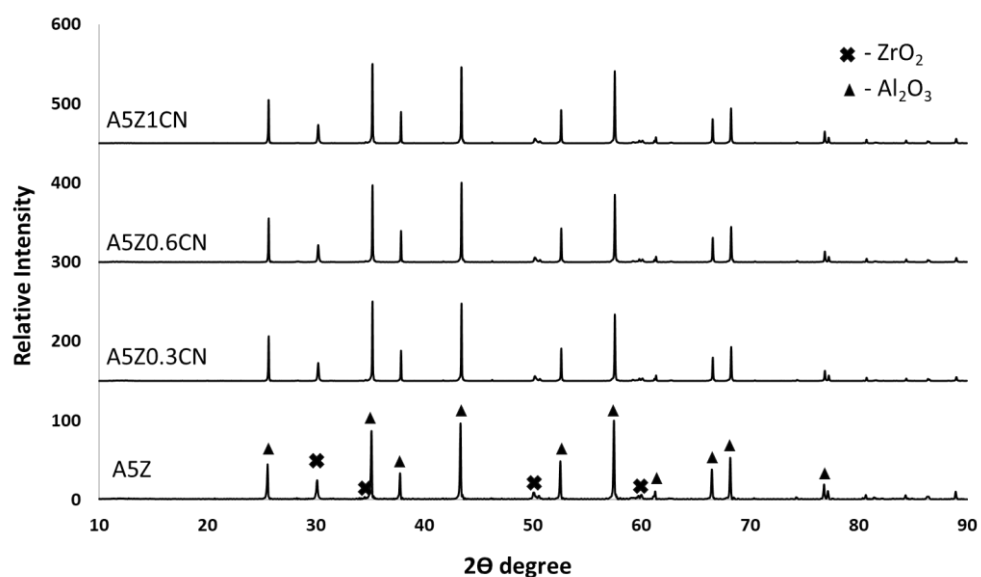


**Figure 2.** XRD patterns of the ZTA and ZTA- $\text{Cr}_2\text{O}_3$  composites after sintering prepared with nano  $\text{Cr}_2\text{O}_3$ .

Table 1 shows the relative density values and mechanical properties of the ZTA and ZTA- $\text{Cr}_2\text{O}_3$  composites. Due to the vaporization-condensation sintering character of  $\text{Cr}_2\text{O}_3$ , it is challenging to determine the exact relative density values of  $\text{Cr}_2\text{O}_3$  containing composites (Zhao et al., 2018). Therefore, in this study, the relative densities of ZTA- $\text{Cr}_2\text{O}_3$  composites were calculated using the rule

of mixtures for comparison purposes only. The relative densities decreased slightly with the addition of  $\text{Cr}_2\text{O}_3$  to the ZTA composite except for the composite containing 0.3  $\text{Cr}_2\text{O}_3$  prepared with micron powder. This situation is thought to be within the experimental error that in general, all relative density values were close to each other for the  $\text{Cr}_2\text{O}_3$  containing composites. This situation is also reflected in the elastic modulus values. In general, higher densification results in higher elastic modulus for the same material (Kafkaslıoğlu Yıldız et al., 2019; Wanner, 1998; Feng et al., 2019). In this case, the relative elastic modulus values must be considered. The elastic modulus is around 200 GPa for the tetragonal phase in zirconia ceramics, 400 GPa for pure  $\text{Al}_2\text{O}_3$  and 280 GPa for  $\text{Cr}_2\text{O}_3$  (Broniszewski et al., 2013; Lu et al., 2003). Adding a component with a lower elastic modulus to the ceramic body will lower the overall elastic modulus. Since there is the same amount of  $\text{ZrO}_2$  in all the composites and they are close to each other at the point of densification, the elastic modulus values are slightly lower than ZTA but close to each other for the  $\text{Cr}_2\text{O}_3$  containing composites.  $\text{Cr}_2\text{O}_3$  is not considered a separate phase as it is completely dissolved. Therefore, its effect on densification is also reflected in the elastic modulus.

**Table 1.** The mechanical properties of the ZTA and ZTA- $\text{Cr}_2\text{O}_3$  composites

Composition	Relative Density (%)	Elastic Modulus (GPa)	$\text{Al}_2\text{O}_3$ Grain Size ( $\mu\text{m}$ )	Hardness (GPa)	Flexural Strength (MPa)
A5Z	97.0 ± 1.2	370 ± 9	3.23	19.5 ± 1.2	317 ± 77
A5Z0.3C	97.3 ± 1.0	368 ± 9	3.31	18.9 ± 0.5	281 ± 57
A5Z0.6C	96.7 ± 1.2	364 ± 16	3.56	19.6 ± 1.6	339 ± 76
A5Z1C	96.5 ± 1.4	357 ± 16	3.35	18.9 ± 1.1	327 ± 93
A5Z0.3CN	96.4 ± 1.0	361 ± 13	3.06	19.3 ± 2.2	240 ± 37
A5Z0.6CN	96.7 ± 1.0	361 ± 12	3.02	20.0 ± 0.8	299 ± 37
A5Z1CN	96.8 ± 0.9	363 ± 10	2.82	20.7 ± 0.5	299 ± 54

Figure 3 shows the thermally etched SEM images of ZTA and ZTA- $\text{Cr}_2\text{O}_3$  composites both prepared with nano and micron-sized  $\text{Cr}_2\text{O}_3$  powder. YSZ grains are represented by the white areas, and  $\text{Al}_2\text{O}_3$  grains are represented by the grey areas. Also, the  $\text{Al}_2\text{O}_3$  matrix grain sizes are given in Table 1.  $\text{ZrO}_2$  particles are well distributed in the matrix mainly at grain boundaries and triple junctions and almost no agglomeration was observed. The mean particle size of  $\text{ZrO}_2$  particles was measured as  $\sim 0.80 \mu\text{m}$  in all the composites by using ImageJ software. In parallel with the densification, the matrix grain sizes were also very close to each other and no exaggerated grain growth was detected. The presence of the  $\text{Cr}_2\text{O}_3$  phase cannot be seen individually due to the solid solution formation. Because the complete solid solution of  $\text{Al}_2\text{O}_3$  and  $\text{Cr}_2\text{O}_3$  without the occurrence of any eutectic have a crystal structure resembling corundum (Zhao et al., 2018). Nonetheless, the SEM-EDX mapping data in Figure 4 can be used to demonstrate the existence of  $\text{Cr}^{3+}$ . Dark black areas are oxygen, turquoise areas are aluminum, yellow point areas are zirconium, and pink areas are chromium in the figure. The mapping results roughly prove that  $\text{Cr}_2\text{O}_3$  dissolved in the  $\text{Al}_2\text{O}_3$  matrix.

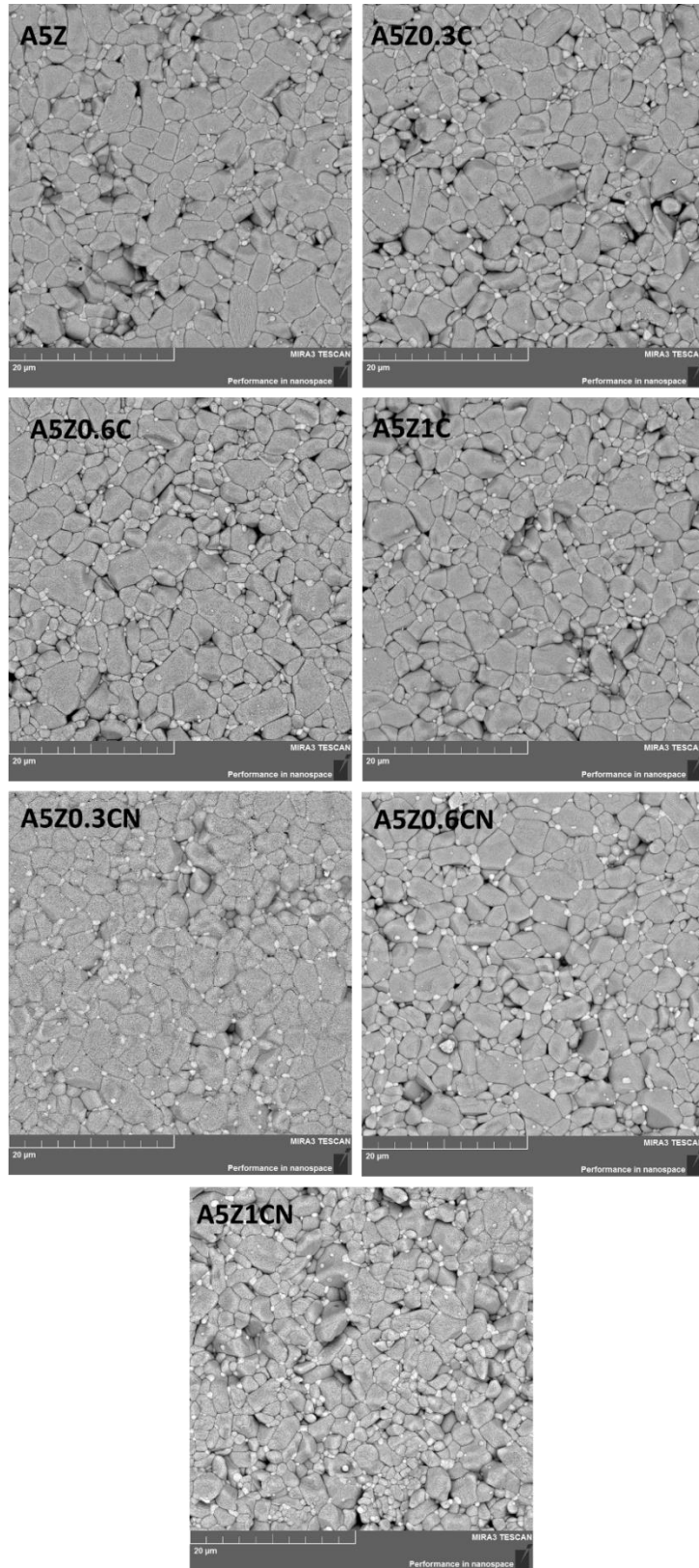


**Figure 3.** SEM images of thermally etched ZTA and ZTA-Cr<sub>2</sub>O<sub>3</sub> composites (the scale is 20 μm)

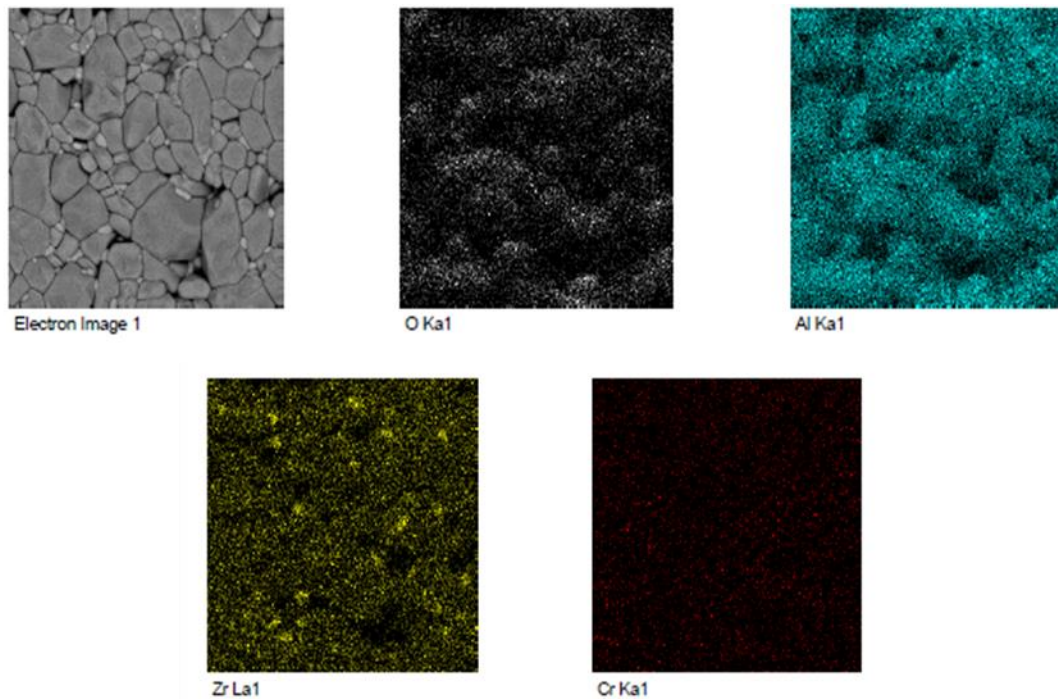


**Figure 4.** SEM-EDS mapping images of ZTA-Cr<sub>2</sub>O<sub>3</sub> composites

In Figure 5 and Table 1, Vickers hardness values are also given. It was observed that the addition of Cr<sub>2</sub>O<sub>3</sub> did not have a serious effect on the hardness of ZTA composites by taking into account the standard deviations. This closeness in hardness values can be explained by the similar-sized Al<sub>2</sub>O<sub>3</sub> grains, the same ZrO<sub>2</sub> content and the similar densification for all the composites. On the other hand, a hardness increase was seen in ZTA-Cr<sub>2</sub>O<sub>3</sub> composites prepared with nano-sized Cr<sub>2</sub>O<sub>3</sub> powder by increasing Cr<sub>2</sub>O<sub>3</sub> content. Again, considering the standard deviations and low relative densities, it is thought that this increase is not very significant. On the other hand, an increase in hardness could be expected after the solid solution formation due to the grain boundary strengthening that generates the hardening of the matrix by inhibiting the permanent deformation and microcracking (Riu et al., 2000; Azhar et al., 2012; Kafkaslıoğlu Yıldız et al., 2019; Rondinella et al., 2021). In order to see the exact effect of the Cr<sub>2</sub>O<sub>3</sub> additive on hardness, it is necessary to examine the Cr<sub>2</sub>O<sub>3</sub> content in different sintering conditions and a wider range of amounts.

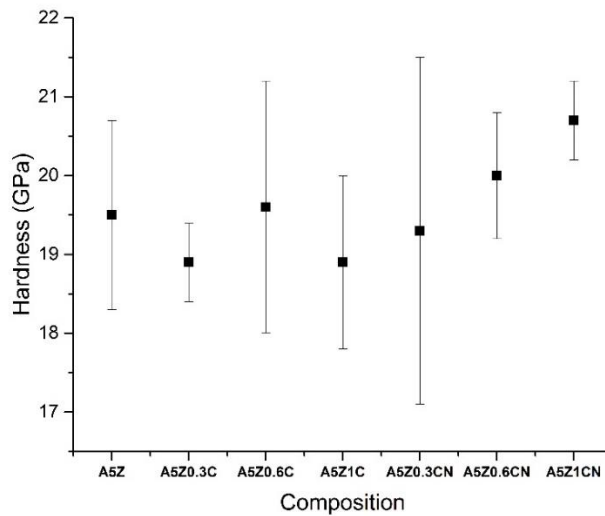


**Figure 5.** The Vickers hardness relation of the composites up to the composition

In this study, the main effect of  $\text{Cr}_2\text{O}_3$  addition on ZTA composites was seen for flexural strength. The flexural strength values are given both in Table 1 and Figure 6. The highest strength value was obtained for A5Z0.6C at 339 MPa. Standard deviations were high in all composites due to the structural defects generated in processing. Compared to the ZTA, a nearly 7% increase is present for A5Z0.6C. Nevertheless, nano-sized  $\text{Cr}_2\text{O}_3$  addition to the ZTA composite negatively affected the strength values. In composites prepared with nano-sized  $\text{Cr}_2\text{O}_3$  powder, the strength values for all ratios are lower than ZTA. Normally, in composites prepared with nano-sized powder, it would be expected that the solid solution would show more positive effects on mechanical properties with more surface area and ultimately more solid solution formation. However, it is seen that the direct addition of nano-sized powder is not effective since the powder does not disperse homogeneously during the process by probable agglomeration, and does not create a homogeneous solid solution formation in the microstructure. Therefore, instead of using nanopowder directly, using a precursor such as  $\text{Cr}(\text{NO}_3)_3 \cdot 9\text{H}_2\text{O}$  instead of nanopowder or a larger-sized powder seems appropriate while processing (Xia et al., 2016).

The increase of flexural strength in A5Z0.6C and A5Z1C composites compared to the A5Z composite can be based on the generated compressive stresses in the grain boundary leads to strengthening (Lin et al., 2012; Kafkaslıoğlu Yıldız et al., 2019; Li et al., 1999). In Li et al. study, an increase in flexural strength was also obtained after 0.4 mol%  $\text{Cr}_2\text{O}_3$  addition to the pure  $\text{Al}_2\text{O}_3$  and the increase was attributed to the grain boundary modification produced by the bigger size of the  $\text{Cr}^{3+}$  ions substituting  $\text{Al}^{3+}$  ions comes out localized compressive stresses (Li et al., 1999). On the other hand, localized compressive stresses caused by ion dimension misfit begin to overlap with rising  $\text{Cr}_2\text{O}_3$  quantity and its positive effect reduces. The decrease in the strength value for A5Z1C compared to A5Z0.6C may be due to this effect.

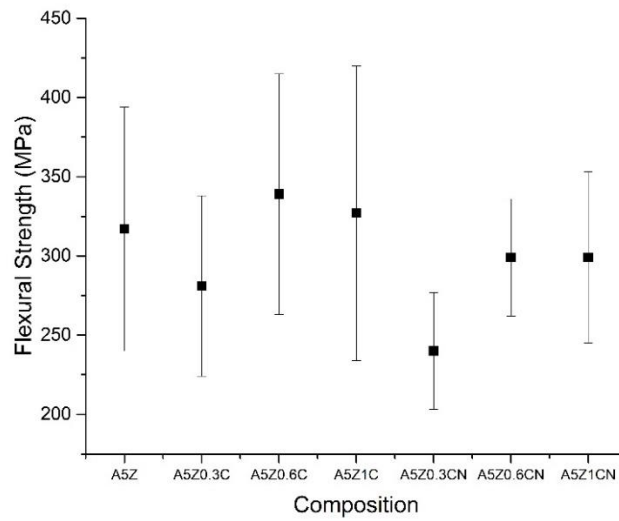


**Figure 6.** The flexural strength relation of the composites up to the composition

Figure 7 shows the photographs of ZTA and ZTA-Cr<sub>2</sub>O<sub>3</sub> composites taken after the strength tests. ZTA composites seem white while ZTA-Cr<sub>2</sub>O<sub>3</sub> composites seem pink in colour. The original colour of the Cr<sub>2</sub>O<sub>3</sub> powder is green. Depending on the chromium level, colouring might range from green to red after sintering (Nguyen et al., 2017). Cr<sub>2</sub>O<sub>3</sub> level must be higher than Al<sub>2</sub>O<sub>3</sub> content in order to produce a green colouring pigment. Due to the lower ion size of Al<sup>3+</sup> as compared to Cr<sup>3+</sup>, the crystal field expands as the aluminum concentration rises. This results in a shift in the absorption bands to higher energies and a pink colour, which is the case for rubies (Munoz et al., 2004). The colouration of Cr<sup>3+</sup> alters with its amount from purple to purplish red in Al<sub>2</sub>O<sub>3</sub> (Bernardi et al, 2004). The colour of the composite changed to darker pink with increasing Cr<sub>2</sub>O<sub>3</sub> content in the ZTA-Cr<sub>2</sub>O<sub>3</sub> composites as seen in Figure 6.

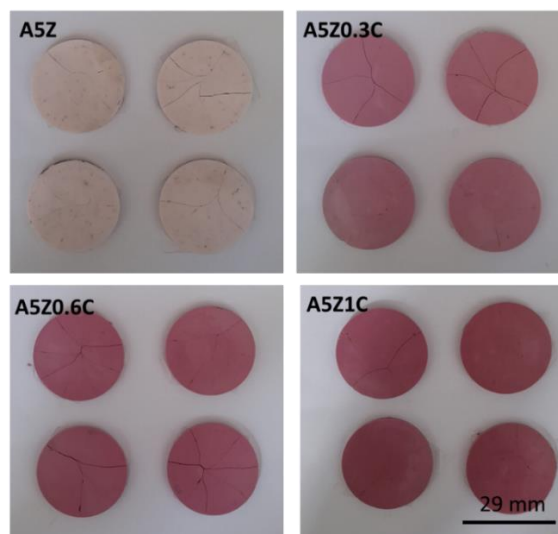


**Figure 7.** Photographs of ZTA and ZTA-Cr<sub>2</sub>O<sub>3</sub> composites taken after strength testing.

## **Conclusion**

In this study, the effects of  $\text{Cr}_2\text{O}_3$  addition on densification and mechanical properties (elastic modulus, hardness, and flexural strength) of ZTA composites were investigated. Processing involved separately adding nano and micron-sized  $\text{Cr}_2\text{O}_3$  powder to the ZTA composite in weight ratios of 0.3, 0.6, and 1%, followed by uniaxially dry pressing immediately after pressureless sintering at  $1650^\circ\text{C}$  for two hours in the air.  $\text{ZrO}_2$  particles are well distributed in the matrix mainly at grain boundaries and triple junctions and almost no agglomeration was observed. Due to the solid solution formation, the  $\text{Cr}_2\text{O}_3$  additive was not seen as a separate phase in both XRD and SEM results. For the composites containing  $\text{Cr}_2\text{O}_3$ , the relative densities of all the materials were rather close to one another. Due to the evaporation problem, a small reduction in both densification and elastic modulus was seen with the addition of  $\text{Cr}_2\text{O}_3$ . Moreover, the hardness of the ZTA composites was not significantly affected by the addition of  $\text{Cr}_2\text{O}_3$ . The flexural strength of ZTA composites was the main outcome of  $\text{Cr}_2\text{O}_3$  addition. The direct addition of nano-sized powder is ineffective as the powder does not distribute uniformly during the process, possibly due to agglomeration, and does not result in a homogeneous solid solution formation in the microstructure. Due to the generated compressive stresses in the grain boundary caused by solid solution formation, 0.6wt% $\text{Cr}_2\text{O}_3$  containing composite prepared with micron sized  $\text{Cr}_2\text{O}_3$  powder showed a roughly 7% improvement in strength when compared to the ZTA. Eventually, ZTA composite containing 0.6wt%  $\text{Cr}_2\text{O}_3$  additive with high strength value (339 MPa) can be possible used as an alternative material to ZTA composites for critical structural applications demanding high strength.

## **Acknowledgements**

This article was prepared from the studies of Uğur Usta for his master's degree at Sivas University of Science and Technology, Defense Technology Program. The authors thank Dr Besim Gökçe Dara in Roketsan for his collaboration in the thesis. The authors also thank Halil İbrahim Çetintaş and Adem Şen for their assistance in the SEM and XRD analysis of this study, respectively.

## **Conflict of Interest Statement**

The article's authors declare that there is no conflict of interest.

## **Contribution Rate Statement Summary of Researchers**

UU carried out the experiments and the theoretical calculations with BKY. BKY wrote the article and UU contributed to the interpretation. All authors have read and agreed to the final version of the article.

## References

- Arahor T., Whitney ED. Microstructure and mechanical properties of  $\text{Al}_2\text{O}_3\text{-Cr}_2\text{O}_3\text{-ZrO}_2$  composites. *Journal of Materials Science* 1988; 23: 1605-1609.
- Azhar AZA., Choong LC., Mohamed HM., Ratnam MM., Ahmad ZA. Effects of  $\text{Cr}_2\text{O}_3$  addition on the mechanical properties, microstructure and wear performance of zirconia-toughened-alumina (ZTA) cutting inserts. *Journal of Alloys and Compounds* 2012; 513: 91–96.
- Azhar AZA., Mohamad H., Ratnam MM., Ahmad ZA. The effects of MgO addition on microstructure, mechanical properties and wear performance of zirconia-toughened alumina cutting inserts. *Journal of Alloys and Compounds* 2010; 497: 316–320.
- Bernardi MIB., Crispim SCL., Maciel AP., Souza AG., Conceição MM., Leite ER., Longo E. Synthesis and characterization of  $\text{Al}_2\text{O}_3/\text{Cr}_2\text{O}_3$ -based ceramic pigments. *Journal of Thermal Analysis and Calorimetry* 2004; 75: 475–480.
- Broniszewski K., Wozniak J., Czechowski K., Jaworska L., Olszyna A.  $\text{Al}_2\text{O}_3\text{-Mo}$  cutting tools for machining hardened stainless steel. *Wear* 2013; 303: 87–91.
- Chevalier J., Gremillard L., Virkar AV., Clarke DR. The Tetragonal-monoclinic transformation in zirconia: Lessons learned and future trends. *Journal of the American Ceramic Society* 2009; 92: 1901–1920.
- Feng L., Fahrenholtz WG., Hilmas GE., Watts J., Zhou Y. Densification, microstructure, and mechanical properties of ZrC–SiC ceramics. *Journal of the American Ceramic Society* 2019; 102: 5786–5795.
- Hassan AM., Naga SM., Awaad M. Toughening and strengthening of  $\text{Nb}_2\text{O}_5$  doped zirconia/alumina (ZTA) composites. *International Journal of Refractory Metals and Hard Materials* 2015; 48: 338–345.
- Kafkaslioglu Yıldız B., Tür YK. Effect of  $\text{ZrO}_2$  content on the microstructure and flexural strength of  $\text{Al}_2\text{O}_3\text{-ZrO}_2$  composites with the stored failure energy-fragmentation relations. *Ceramics International* 2021; 47: 34199–34206.
- Kafkaslioglu Yıldız B., Yılmaz H., Tür YK. Evaluation of mechanical properties of  $\text{Al}_2\text{O}_3\text{-Cr}_2\text{O}_3$  ceramic system prepared in different  $\text{Cr}_2\text{O}_3$  ratios for ceramic armour components, *Ceramics International* 2019; 45: 20575–20582.
- Li CL., Riu DH., Sekino T., Niihara K. Fabrication and mechanical properties of  $\text{Al}_2\text{O}_3$  solid solution with low addition of  $\text{Cr}_2\text{O}_3$ . *Key Engineering Materials* 1999; 161–163.
- Lin HT., Nayak PK., Liu BZ., Chen WH., Huang JL. Mechanical properties of  $\text{Al}_2\text{O}_3\text{-Cr}_2\text{O}_3/\text{Cr}_3\text{C}_2$  nanocomposite fabricated by spark plasma sintering. *Journal of the European Ceramic Society* 2012; 32: 77–83
- Lu FH., Chen HY., Hung CH. Degradation of CrN films at high temperature under controlled atmosphere. *Journal of Vacuum Science and Technology A* 2003; 21: 671-675.

- Manshor H., Abdullah EC., Azhar AZA., Sing YW., Ahmad ZA. Microwave sintering of zirconia-toughened alumina (ZTA)-TiO<sub>2</sub>-Cr<sub>2</sub>O<sub>3</sub> ceramic composite: The effects on microstructure and properties. *Journal of Alloys and Compounds* 2017; 722: 458-466.
- Manshor H., Azhar AZA., Rashid RA., Sulaiman S., Abdullah EC., Ahmad ZA. Effects of Cr<sub>2</sub>O<sub>3</sub> addition on the phase, mechanical properties, and microstructure of zirconia-toughened alumina added with TiO<sub>2</sub> (ZTA-TiO<sub>2</sub>) ceramic composite. *Int. Journal of Refractory Metals and Hard Materials* 2016; 61: 40-45.
- Moradkhani A., Baharvandi H. Effects of additive amount, testing method, fabrication process and sintering temperature on the mechanical properties of Al<sub>2</sub>O<sub>3</sub>/3Y-TZP composites. *Engineering Fracture Mechanics* 2018; 19: 446-460.
- Munoz R., Maso N., Julian B., Marquez F., Beltran H., Escribano P., Cordoncillo E. Environmental study of Cr<sub>2</sub>O<sub>3</sub>-Al<sub>2</sub>O<sub>3</sub> green ceramic pigment synthesis. *Journal of the European Ceramic Society* 2004; 24: 2087-2094.
- Nath M., Kumar P., Maldhure AV., Sinhamahapatra S., Dana K., Ghosha A., Tripathi HS. Anomalous densification behavior of Al<sub>2</sub>O<sub>3</sub>-Cr<sub>2</sub>O<sub>3</sub> system. *Materials Characterization* 2016; 111: 8-13.
- Nguyen DK., Lee H., Kim IT. Synthesis and thermochromic properties of Cr-Doped Al<sub>2</sub>O<sub>3</sub> for a reversible thermochromic sensor. *Materials* 2017; 10: 476.
- Rondinella A., Furlani E., Magnan M., Scagnetto F., Driussi S., Marin E., Maschio S. Synthesis, crystallographic characterization, and mechanical behavior of alumina chromia alloys. 2021; 47: 24494-24500.
- Tuan WH., Chen JR., Ho CJ. Critical zirconia amount to enhance the strength of alumina. *Ceramics International* 2008; 34: 2129-2135.
- Tuan WH., Chen RZ., Wang TC., Cheng CH., Kuo PS. Mechanical properties of Al<sub>2</sub>O<sub>3</sub>/ZrO<sub>2</sub> composites. *Journal of the European Ceramic Society* 2002; 22: 2827-2833.
- Wanner A. Elastic modulus measurements of extremely porous ceramic materials by ultrasonic phase spectroscopy. *Materials Science and Engineering: A* 1998; 248: 35-43.
- Weimin M., Lei W., Renguo G., Xudong S., Xikun L. Sintering densification, microstructure and transformation behavior of Al<sub>2</sub>O<sub>3</sub>/ZrO<sub>2</sub>(Y<sub>2</sub>O<sub>3</sub>) composites. *Materials Science and Engineering A*; 2008: 477: 100-106.
- Xia JF., Nian HQ., Liu W., Wang XG., Jiang DY. Effect of Cr<sub>2</sub>O<sub>3</sub> derived from Cr(NO<sub>3</sub>)<sub>3</sub>·9H<sub>2</sub>O precursor on the densification and mechanical properties of zirconia-toughened alumina (ZTA) composites. *Ceramics International* 2016; 42: 9116-9124.
- Zhao P., Zhao H., Yu J., Zhang H., Gao H., Qi Chen. Crystal structure and properties of Al<sub>2</sub>O<sub>3</sub>-Cr<sub>2</sub>O<sub>3</sub> solid solutions with different Cr<sub>2</sub>O<sub>3</sub> contents. *Ceramics International* 2018; 44: 1356-1361.